

Challenges in high-intensity laser injection into multiple optical fibers

Robert E. Setchell and Dante M. Berry

Sandia National Laboratories, MS1421, Albuquerque, New Mexico 87185

ABSTRACT

A growing number of applications involve the transmission of high-intensity laser pulses through optical fibers. Previously, our particular interests led to a series of studies on single-fiber transmission of Q-switched, 1064 nm pulses from multimode Nd:YAG lasers through step-index, multimode, fused silica fibers. The maximum pulse energy that could be transmitted through a given fiber was limited by the onset of laser-induced breakdown or damage. Breakdown at the fiber entrance face was often the first limiting process encountered, but other mechanisms were observed that could result in catastrophic damage at either fiber face, within the initial “entry” segment of the fiber, and at other internal sites along the fiber path. These studies examined system elements that can govern the relative importance of different damage mechanisms, including laser characteristics, the design and alignment of laser-to-fiber injection optics, fiber end-face preparation, and fiber routing. In particular, criteria were established for injection optics in order to maximize margins between transmission requirements and thresholds for laser-induced damage. Recent interests have led us to examine laser injection into multiple fibers. Effective methods for generating multiple beams are available, but the resulting beam geometry can lead to challenges in applying the criteria for optimum injection optics. To illustrate these issues, we have examined a three-fiber injection system consisting of a beam-shaping element, a primary injection lens, and a grating beamsplitter. Damage threshold characteristics were established by testing fibers using the injection geometry imposed by this system design.

Keywords: high-intensity fiber transmission, multiple-fiber laser injection, laser damage in optical fibers

1. INTRODUCTION

Applications in medicine, material processing, telecommunications, and defense technologies are motivating studies of high-intensity laser transmission through optical fibers.^{1,2} Our studies began in the late 1980s, motivated by the possibility of developing methods for initiating explosives that were inherently safe from accidental electrical currents. These studies persisted for more than a decade, typically using Q-switched, multimode Nd:YAG lasers and relatively large step-index, fused silica fibers. A number of laser-induced damage mechanisms were encountered that would limit the pulse energy that could be transmitted, and methods to mitigate these mechanisms became a focus of our studies. Once optimum methods for fiber end-face processing were identified, the important role of laser-to-fiber injection optics became our primary interest. Criteria for injection optics were developed to maximize margins with respect to damage thresholds. The culmination of this period of study was the incorporation of custom beam-shaping optics to achieve our highest damage thresholds for compact, single-fiber injection.

The many applications for high-intensity fiber transmission that have developed in recent years have rapidly expanded the range of associated laser types and operating characteristics, as well as the types of fibers in use. Our renewed interests have not varied substantially from past studies in terms of laser and fiber types, but have led us to consider multiple-fiber transmission systems and the issues that arise as the number of fibers increases. The present study examines these issues in the context of the criteria developed previously for optimum single-fiber injection. The following background section reviews the different damage mechanisms that can occur in fibers, and the system elements that can affect which mechanisms ultimately limit fiber transmission. The criteria for optimum injection optics are identified, and the various efforts that were made to implement the criteria are summarized. The next section discusses the challenges that arise in trying to apply these criteria to the design of multiple-fiber injection optics, and briefly describes a previous study that addressed these issues. The fourth section presents a particular design for a three-fiber injection system, and describes the fiber testing that was conducted to establish the damage threshold characteristics of this system. The results are discussed in the final section.

2. BACKGROUND

For a number of years we investigated single-fiber transmission of Q-switched pulses from multimode Nd:YAG lasers operating at 1064 nm. Step-index, multimode fibers of interest had relatively large cores (diameter $\geq 365 \mu\text{m}$) of pure fused silica. We found that a number of laser-induced damage mechanisms were possible, and that various system elements could affect the onset of particular mechanisms. This section briefly reviews the insights gained during the course of these studies.

2.1 Laser-induced damage mechanisms in optical fibers

As the pulse energy injected into a fiber is increased, fiber transmission is eventually interrupted by a laser-induced breakdown or damage mechanism. Various mechanisms have been identified,³ as illustrated in Fig. 1. Of these mechanisms, the first to limit fiber transmission is often a plasma-forming breakdown at the fiber entrance face. This breakdown can result in subtle surface modifications that leave the fiber face more resistant to breakdown or damage in subsequent laser pulses. We denote this process as breakdown rather than damage to distinguish it from a plasma-forming event on the entrance face in which small pits form on the surface, and subsequent laser pulses simply produce more violent events with more extensive pitting. In either case, the formation of an absorptive plasma at the entrance face results in a significant reduction in the transmitted pulse energy. If entrance-face breakdown or damage does not occur during a high-intensity laser pulse, catastrophic damage can occur at the fiber exit face, within the initial "entry" segment of the fiber path, or at other internal sites related to fiber routing. A much smaller loss in transmitted energy typically occurs during a pulse that results in one of these damage processes.

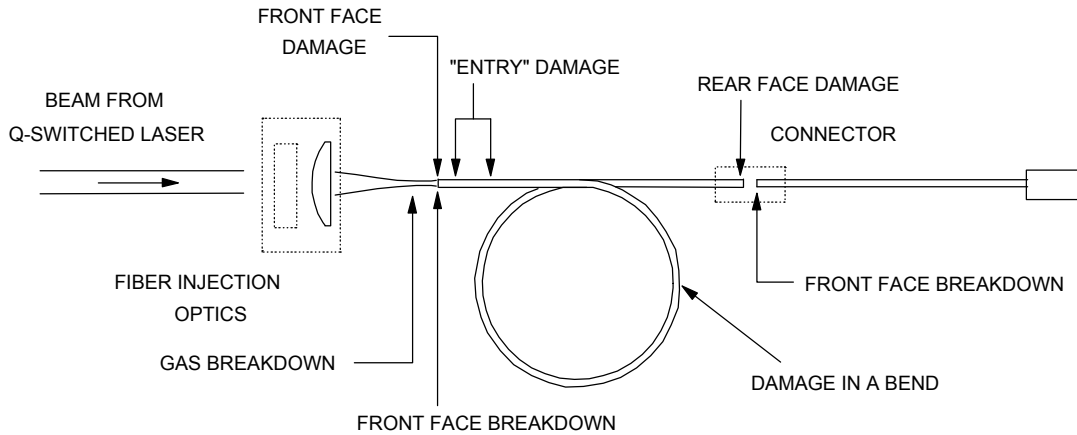


Fig. 1 Breakdown and damage processes in a high-intensity fiber transmission system

For a given laser and fiber combination, we found that the particular breakdown or damage mechanisms that ultimately limit fiber transmission can depend on the following system elements: laser characteristics, the design and alignment of laser-to-fiber injection optics, fiber end-face preparation, and fiber routing.³ Entrance-face breakdown and damage depend on the surface characteristics resulting from end-face preparation processes, and on the peak laser fluence at this face resulting from laser characteristics and the laser-to-fiber injection optics. The relative merits of different end-face preparation processes such as cleaving, mechanical polishing, and conditioning with a CO₂ laser have been addressed in a number of previous investigations.³⁻⁶ A particular schedule for CO₂-laser conditioning following a good mechanical polish produced surfaces that were highly resistant to breakdown or damage.^{3,6} The other factor affecting entrance-face breakdown and damage thresholds depends on the relation between the peak local fluence at this surface and the total laser energy incident on the fiber core. By use of magnified beam-profiling techniques, the nominal fluence distribution on a fiber entrance face resulting from a particular combination of laser and injection optics can be established. A figure of merit for laser conditions at the entrance face can be defined by the following ratio of peak to average fluences:

$$P/A = \frac{\text{peak local fluence}}{(\text{total energy incident on fiber core})/(\text{fiber core area})}$$

A perfect “flat top” fluence distribution extending over the entire core area would achieve a value of unity for this ratio. In practice, using different lasers and injection optics, we have observed values for this ratio varying from less than 3 to more than 5. The highest values have resulted from simple lens injection of multimode lasers with strong “hot spots”. When using simple lens injection in our early studies, we found it necessary to modify a commercial multimode laser used in our testing in order to produce a more benign beam profile. The maximum possible spot size on the fiber entrance face is governed by the need to prevent light from entering the cladding layer, and will depend on the accuracy of the method used to align the fiber axis with the axis of the laser beam. Light injected into the cladding can be absorbed by the material used to bond stripped fiber in a support fixture or connector, or by the fiber buffer material. If sufficient energy is absorbed locally, structural damage can occur that ultimately leads to fiber transmission failure.

Damage beyond the entrance face but within the initially straight portion of the fiber path is denoted as “entry” damage. This damage occurs when initial reflections along the core/cladding interface result in internal beam focusing, with very high local fluences produced within one or more fiber cross sections within the “entry” region. In general, a great many reflections over a considerable length of fiber are necessary before a reasonably steady fluence distribution can be established in fiber cross sections.⁷ Damage sites can appear near the core/cladding interface or nearly centered within the core, depending on the focusing pattern. Early studies⁸⁻¹⁰ found that “entry” damage at the core/cladding interface was likely if the laser axis and the initial fiber axis were not collinear. In addition, these studies found that the fiber entrance face should be positioned beyond the focal plane of the injection lens so that the beam will be diverging as it enters the fiber. A larger divergence angle, as produced by an injection lens having a shorter focal length, appeared to be desirable provided that air breakdown did not occur at the focal plane. In our studies, however, we have found that satisfying these conditions does not ensure that “entry” damage will be avoided. A radially expanding, axisymmetric beam closely centered about the fiber axis can be refocused along the axis by reflections at the core/cladding interface, producing periodic damage sites. As will be discussed in the next section, injection optics that generate rays that do not pass through the fiber axis (skew rays) have proven effective in avoiding this particular damage process.

The divergence and intensity distribution of the beam entering the fiber entrance face define the initial mode power distribution within the fiber. With respect to meridional rays (rays that pass through the fiber axis), the mode power distribution is a description of how the total laser power is distributed relative to the angle that rays make with the axis,⁷ with the maximum possible angle corresponding to the critical angle for total internal reflection at the core/cladding interface (which determines the fiber’s numerical aperture, or NA). Unless an injection lens with a very short focal length is used, the initial mode power distribution may only extend to an angle much smaller than the maximum angle. This condition of “low NA” injection will increase the likelihood of “entry” damage at the core/cladding interface if the fiber axis is not aligned to be collinear with the incident beam axis. Even with good alignment, this condition can lead to a persistent damage mechanism within the first major bend along the fiber path. In previous studies using simple lens injection, internal damage was often observed within a fiber segment that had transitioned from a straight entrance path to a constant-radius bend that continued through a 360° loop. This damage resulted from very high fluences in the outside portion of the fiber cross section (away from the center of curvature). Although any bend in the fiber path will cause the mode power distribution to become asymmetric, the extreme asymmetry in this case was due to a significant portion of the total energy being confined to “whispering gallery” rays¹¹ that only reflect from the outer core/cladding boundary. To inhibit this damage process, the mode power distribution must be relatively broad prior to the first bend in the fiber path. In one study, the occurrence of damage in the initial bend was reduced by using a mechanical mode scrambler in the “entry” segment following simple lens injection.³ More recent studies have essentially eliminated this damage mechanism by using injection optics that include both a primary lens with a very short focal length and a beam-shaping element that prevents strong focusing in the focal plane of this lens.¹²

An additional damage mechanism related to fiber routing was observed in previous studies at positions along the fiber path where the fiber was forced to experience a small bending radius locally. Such a condition can be introduced inadvertently when a fiber is routed around a thin post or sharp edge and then some axial tension is applied. Susceptibility to this damage mechanism is enhanced if the fiber only has a thin buffer and no additional protective layers. In most cases no loss in transmission was observed prior to damage, suggesting that the locally imposed geometry was causing focusing within the fiber core. Damage related to localized path deviations can also result from fiber fixturing. Careless fixturing of 20 fibers in one study¹³ resulted in every fiber damaging at nearly the same location within the “entry” segment at relatively low energies. Use of a high-shrinkage epoxy apparently caused the path of each fiber to be locally distorted.

The damage mechanism at the fiber exit face is different from that at the entrance face. Assuming that a reasonably good surface finish has been achieved through polishing, damage at the exit face will typically result from subsurface defects remaining from early polishing steps.¹⁴ We have also observed exit face damage with cleaved surfaces due to subsurface fractures created during the cleaving process.⁵ This dependence on subsurface features for exit face damage results from a standing wave pattern during the laser pulse that produces peak intensities at discrete depths into the silica.¹⁵ Exit face damage typically results in one or more large craters that start from the depth where the damage initiates. Subsurface defects are difficult to detect and can be present even if the final surface finish is very good. Minimizing this damage mechanism depends on developing a careful polishing schedule in which sufficient material is removed at each step.

2.2 Criteria for optimum fiber injection optics, and implementation efforts

As discussed in the previous section, different system elements can be important in determining the onset of various breakdown and damage mechanisms. The design and alignment of injection optics directly affect the onset of entrance face breakdown and damage, “entry” damage, and damage at an initial bend in the fiber path. An optimum design for injection optics would inhibit these processes by minimizing peak local fluences on the fiber entrance face, by immediately generating a broad mode power distribution in the fiber, and by preventing refocusing patterns within the “entry” segment of the fiber path. An additional attribute would be insensitivity to small alignment errors between the optical elements. In applications requiring the use of highly multimode lasers that can have strong “hot spots” in the beam and significant pulse-to-pulse variations, these design criteria are obviously very challenging. During our early studies it quickly became apparent that simple lens injection would not provide adequate margins with respect to damage thresholds.

An initial approach beyond simple lens injection that actually produced very high damage thresholds was a rather cumbersome, “fiber-to-fiber” injection system.⁴ A lens with a 50-mm focal length was used to inject the output from a test laser into a length of fiber having a diameter of 600 μm and a numerical aperture of 0.11. This fiber had a number of 360° loops in its path to mix the fiber modes. The output of this fiber was imaged with demagnification optics onto test fibers having a core diameter of 400 μm and a numerical aperture of 0.22. Fiber end faces were mechanically polished followed by conditioning with a CO₂ laser, and 16 out of 17 test fibers did not breakdown or damage before reaching the laser’s maximum possible transmitted energy of 100-105 mJ. This configuration came reasonably close to an ideal fiber injection condition in which the initial mode power distribution at the fiber entrance face would be comparable to an equilibrium distribution established after a very long fiber path.⁷

We began developing diffractive optical elements as components for more compact fiber injection optics in 1993. The first design was a multiple-order diffractive axicon that distributed the laser beam over a number of concentric rings on the fiber entrance face.¹⁶ This design successfully mitigated “hot spots” and provided control of the fluence distribution over the fiber face, achieving lower values for the ratio of peak to average fluences on this face than could be achieved with simple lens injection. This element was combined with a lens having a short focal length, resulting in a broad mode power distribution in the fiber. The fiber entrance face was positioned at the focal plane of this lens, where peak fluences were much smaller than fluences that would result from using the lens alone. Alignment of the diffractive element with the laser beam and lens was relatively insensitive. Unfortunately, this design produced a refocusing pattern within the “entry” segment of the fiber, and catastrophic damage occurred at evenly spaced sites along the fiber axis at relatively low pulse energies.¹⁷ Subsequently, three more diffractive elements were progressively designed, fabricated, and tested at Sandia National Laboratories for use in injection optics. These designs addressed the problem of refocusing patterns within the “entry” segment by introducing diffraction angles in planes that were perpendicular to the radial direction in these elements. When combined with the radial focusing produced by a conventional lens, skew rays that do not pass through the fiber axis are transmitted into the fiber. The last of these designs was successful in addressing all of the criteria for injection optics, and has been used extensively in our studies of high-intensity fiber transmission.^{5,6,12} This diffractive optic is combined with a plano-convex lens having a very short focal length (15.2 mm).

As shown in Fig. 2, this 6-mm-diameter design is composed of 87 individual segments arranged within 5 concentric rings. Each segment is a low-spatial-frequency grating that diffracts the incident light into plus and minus first and second orders. The diffraction pattern is achieved through a 14-level structure etched into a fused silica substrate.

Within each segment the orientation of the grating is approximately radial, and the diffraction angles are in a plane perpendicular to this orientation. A number of skew angles are generated by having different diffraction angles at different radial positions. The final intensity distribution at the focal plane of the lens results from the superposition of the diffraction patterns produced by each individual segment. Most of these patterns do not overlap in the focal plane, minimizing possible interference effects. Parameters in the design of this element were the diffraction angles, the percentage of incident light going into each order, and the geometric arrangement of the segments. These parameters permit considerable control of the fluence distributed over a fiber entrance face positioned at the focal plane of the lens. The light incident upon a particular segment appears at four locations on the fiber face, with spacings that correspond to the product of the focal length and the diffraction angles. This actively mitigates a “hot spot” in the laser near-field profile that falls on one or more of the diffractive segments. This design has resulted in our lowest measured values to date for the ratio of peak to average fluences on the fiber entrance face. As expected, the use of a lens having a very short focal length produces a broad initial mode power distribution in the fiber, and the skew angles introduced by the diffractive segments prevent refocusing patterns within the “entry” segment. In all of our studies, the highest damage thresholds for compact, single-fiber injection were achieved when we used this optic with fibers having superior end-face preparation.⁶ The only disadvantage of this design is its relatively low transmission efficiency. Even with anti-reflection coatings, light diffracted into higher orders and light scattered at the etched silica surface result in a 16% loss in light transmitted into a fiber core.

A design for injection optics with higher transmission efficiency combines a plano-convex lens having a short focal length (17.1 mm) with a custom beam-shaping optic consisting of a two-dimensional array of hexagonal lenslets.¹⁸ A photograph of a portion of this optic is shown in Fig. 3. Approximately 20 lenslets are contained within an overall

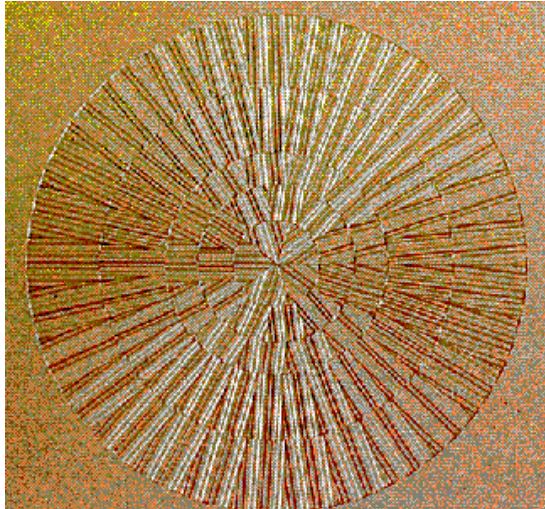


Fig. 2 Concentric rings containing individual diffractive elements

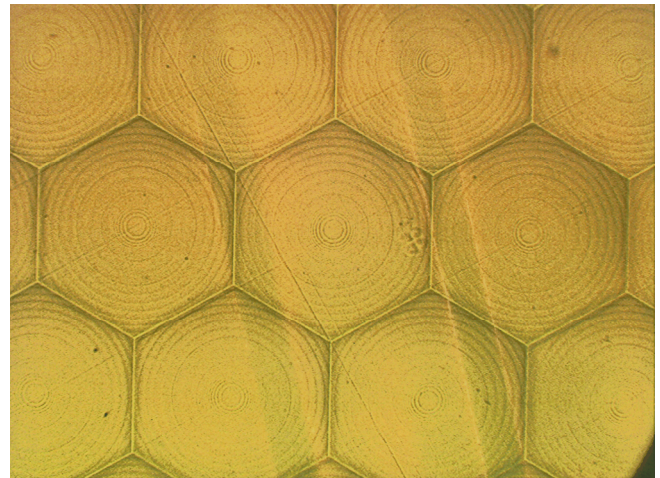


Fig. 3 Hexagonal lenslet array

diameter of 8 mm, with each lenslet having an edge-to-edge dimension of 1.25 mm. The lenslets are refractive with a focal length of 69 mm. An incident laser beam first strikes the lenslet array, where it is segmented into multiple beamlets. After passing through the primary injection lens, each beamlet passes through a focus and then forms a spot having a desired diameter at the focal plane of this lens. The spot diameter is chosen to be approximately 85% of the core diameter of a fiber whose entrance face is positioned at this focal plane. The spots from the different beamlets overlap, and the final intensity distribution on the fiber entrance face during a laser pulse results from the superposition of these individual contributions. A brief theoretical analysis of focal plane fluences produced by this design, and a detailed experimental characterization of these fluences, have been reported.¹⁸ Diffraction effects from the finite lenslet dimensions result in a coarse modulation of the fluence profile appearing in the focal plane. Stronger, more closely spaced profile fluctuations result from interference between superimposed beamlets. The degree of interference depends on the coherence properties of the particular laser beam. For a given fiber spot size and primary lens focal length (chosen to nearly fill the fiber’s numerical aperture), the remaining design parameter is the lenslet diameter (the ratio of

lenslet focal length to diameter will be fixed). The lenslet diameter can be reduced in order to divide the laser beam into more overlapping beamlets, but diffraction and interference effects on the final profile will be enhanced.

This design mitigates “hot spots” in the laser beam very effectively by dividing the cross-sectional area of the beam into smaller segments and then superimposing each of these segments over a common area filling most of the fiber core. Unless interference effects are dominant, this approach will result in much lower values for the ratio of peak to average fluences on the fiber entrance face than could be achieved with simple lens injection. The initial experimental evaluation of this design¹⁸ achieved low (≤ 3) peak-to-average ratios that were insensitive to alignment errors. The use of a primary injection lens with a very short focal length obviously produces a broad mode power distribution in the fiber. An efficiency of 96.4% for fiber injection was measured for the lenslet array, which has anti-reflection coatings on both surfaces. The primary disadvantage to this design is that it is susceptible to damage due to refocusing in the “entry” segment of the fiber. Our damage threshold testing with this design resulted in 9 out of 20 fibers damaging within the “entry” segment of the fiber path.¹² The damage sites were periodically spaced along the fiber axis, indicative of a radial refocusing pattern. These results will be discussed further in Section 4.

In summary, our studies of high-intensity laser transmission through single fibers resulted in certain criteria for optimum injection optics: minimize peak local fluences on the fiber entrance face, immediately generate a broad mode power distribution in the fiber, and prevent refocusing patterns within the “entry” segment of the fiber path. Successfully addressing all of the criteria is difficult, although we eventually achieved very good results using custom beam-shaping optics.

3. MULTIPLE-FIBER INJECTION

Our current interests have led us to consider laser injection into multiple fibers. The additional challenges that can arise in trying to achieve high damage thresholds while injecting into multiple fibers will be discussed, and a brief description will be given of a past program that addressed these issues.

3.1 Challenges

In an application which requires a high-intensity laser pulse to be transmitted through multiple fibers, the criteria for optimum injection optics must be addressed while incorporating a beam distribution system. The simplest distribution system generates multiple beams using a series of beam splitters followed by a mirror.¹⁹ The resulting beams are parallel and displaced some distance from each other, and single-fiber injection optics are used for each beam. Although this approach introduces no new injection issues, it requires an increasing amount of space and optics for every additional output fiber.

An approach that can be extended to many more fibers is to use a diffractive grating to produce a one-dimensional or two-dimensional array of diverging beams. Design issues for the grating include diffraction efficiency and energy balance between diffraction orders. Challenges to achieving optimum injection into a corresponding array of fibers arise due to the geometry of the resulting beam pattern. The simplest approach is to use a lens prior to the grating so that an array of focused beams is produced in the focal plane of the lens. The spacing of focused beams is governed by the grating diffraction angles and the position of the grating between the lens and its focal plane. The fiber array is held in a fixture that provides a corresponding spacing between fibers. A fixture designed for attaching fibers having individual connectors will require greater fiber spacing than a fixture that collectively holds all the fibers in a bare state (stripped of polymer buffer layers). The minimum fiber spacing would have bare fibers separated by the diameter of the fiber plus its buffer layers (to avoid having local bending imposed on sections of bare fiber). The simplest fixture to fabricate would hold the fibers with their entrance faces planar and their axes parallel. For a fixture holding bare fibers, this geometry would facilitate the mechanical polishing of all the fibers collectively. Assuming such a fixture is used, a finite angle will be required between the axis of each focused beam and the axis of the corresponding fiber in the array (except for the zero grating order). The maximum angle will be determined by the size of the fiber array and its distance from the diffractive grating. Figure 4 is a sketch of laser injection into a fiber at a finite angle.

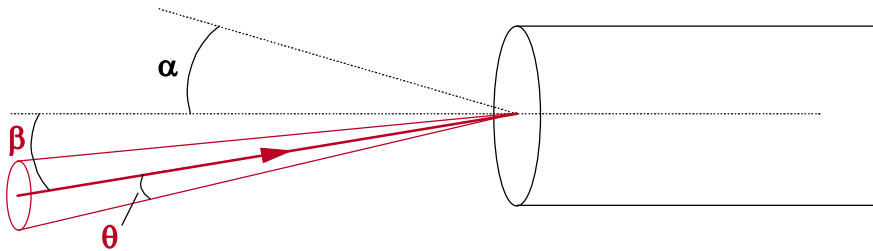


Fig. 4 Laser injection at an angle with respect to the fiber axis

The angle corresponding to the numerical aperture of the fiber is indicated by “ α ” in this figure. The focused beam axis makes an angle “ β ” with respect to the fiber axis, and incoming rays make an angle “ θ ” with respect to the beam axis. For simplicity, consider only rays that are in the plane of this figure. A ray below the beam axis for which $(\beta + \theta) > \alpha$ will not be reflected within the fiber at the core/cladding interface and will pass into the cladding. In addition to a loss in fiber transmission due to incoming rays that exceed the fiber NA, light injected into the cladding can result in events that ultimately lead to transmission failure, as mentioned previously. If the angle β is made larger, the maximum angle θ must be made smaller to avoid this problem. However, this quickly leads to a condition which compromises the criteria for optimum laser injection. Having the maximum value for θ small compared to α corresponds to a condition of “low NA” injection with the beam axis misaligned with respect to the fiber axis. Transmitted pulse energies are now likely to be limited by “entry” damage at the core/cladding interface. In single-fiber injection, this damage mechanism can be mitigated by improved alignment and by using a lens with a shorter focal length to inject at higher angles (ideally with a beam-shaping element to prevent strong focusing and air breakdown). In multiple-fiber injection using a fixture that holds fiber faces planar and their axes parallel, misalignment is intentional and higher injection angles can create problems rather than solve them. Only a more complex approach to holding the fiber array can avoid this difficulty.

3.2 The Lawrence Livermore National Laboratory 16-beam fiber injection system

A program at Lawrence Livermore National Laboratory that accomplished high-intensity laser injection into multiple fibers was reported by Frank *et al.*²⁰ and Honig²¹ in 2000. The initial program goal was to distribute a pulse from a custom 1-Joule, Q-switched laser into 16 fibers to achieve a required pulse energy and smooth profile at the exit of each fiber. Compact size was not a requirement for this system. The multimode, fused silica fibers had a core diameter of 400 μm . The Nd:YLF oscillator/amplifier laser was designed for highly multimode operation in order to deliver a 12 ns pulse at 1047 nm with a nearly top-hat spatial profile and a smooth temporal profile. A sketch of the beam distribution system designed to inject the laser output into a fiber array is shown in Fig. 5. A custom diffractive grating was used to generate 16 beams in a 4×4 pattern, and a lens with a 450 mm focal length was used prior to the grating either to form a de-magnified image of the laser rod on the individual fiber faces or to directly focus the beams just prior to the fiber faces. The fixture for holding the array of fibers was originally designed to accommodate fibers in individual ST connectors, resulting in a fairly large assembly. The resulting injection angles for a simple fixture with parallel fibers were determined to be in excess of a limiting angle, reported as approximately 7°, which resulted in fiber damage at the

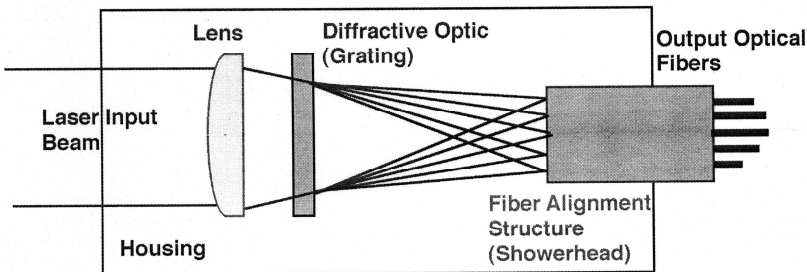


Fig. 5 16-beam fiber injection system (Ref. 20)

core/cladding interface (presumably at the nominal operating pulse energy). Consequently, a spherical structure (the “showerhead” in Fig. 5) having a radius equal to the distance from the grating was used to hold the individual fibers such that each fiber axis was aligned with the axis of its injected laser beam. Alignment of the distribution system components involved precise axial adjustment of lens and grating positions, and rotational adjustment of the grating. These components were mounted in a sealed tube that was aligned as a unit with the laser beam.

In a subsequent design for the beam distribution system, the fiber fixture held bare, polished fibers in a planar, parallel array. At a lens focal length of 500 mm, the resulting injection angles were below 2° . In discussing fiber damage characteristics that were observed when pulse energies were increased, the authors reported that a repeatable failure occurred within 10-15 mm of the fiber entrance faces at the core/cladding interface.

The “entry” damage mechanisms that were encountered in this program reflect the expected challenges in multiple-fiber injection. Since compact size was not a requirement, the overall system design emphasized desirable laser characteristics and utilized lenses with long focal lengths for coupling into the fibers. Despite the fact that this resulted in very “low NA” injection, margins with respect to damage thresholds were sufficient for successful system operation.

4. COMPACT, THREE-FIBER INJECTION OPTICS

Assuming that a diffractive grating will be used for beam distribution, a compact design for laser injection into multiple fibers will probably require compromises to be made between criteria for achieving high damage thresholds and complexity in the fixture that holds the fiber array. An ideal system would use a beam-shaping element, a lens with a short focal length, a diffractive grating, and a fixture similar to the LLNL “showerhead” described previously that holds each fiber entrance face equidistant from the grating and each fiber axis aligned with the corresponding injected beam. Because fabrication of such a fixture could be difficult, it would be useful to know the consequences for damage thresholds and other possible penalties if a simpler fixture were used that held the fiber faces planar and the fiber axes parallel. Relevant factors would include the injection angles involved and the characteristics of the beam-shaping element, but the effects of these factors could only be determined with certainty by testing of the particular design. To illustrate these issues, the experimental evaluation of a design for three-fiber injection will be presented.

4.1 Design

Brown *et al.*²² discussed design issues for a compact, multiple-fiber injection system apart from the laser-induced damage considerations addressed presently. The three-fiber system we have evaluated has similar components, and is shown in Fig. 6. The first element is the same hexagonal lenslet array described in Section 2.2. The second element is a

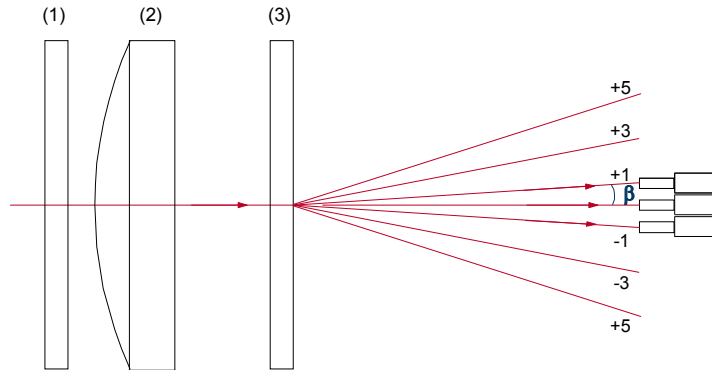


Fig. 6 Three-fiber injection optics. (1): hexagonal lenslet array; (2): 17.1-mm focal length primary lens; (3): diffractive grating. Also shown are higher orders having measurable energies. Fiber core diameter is 365 μm .

plano-convex primary lens with a focal length of 17.1 mm, as used previously with the lenslet array. The final element is a diffractive grating designed to provide nearly equal pulse energies into the zero and \pm first orders. The grating period is chosen to accommodate the required fiber spacing at the focal plane of the lens. The fibers to be used have a core diameter of 365 μm . A prototype of the diffractive grating was fabricated with the intent of having fiber spacing set

at 500 μm , and the performance of this prototype was evaluated in this study. A subsequent grating design is intended to provide a fiber spacing of approximately 750 μm , but fabrication was not completed in time for the present evaluation. The prototype element had a measured diffraction angle β of 3.06° (Fig. 6), with higher order modes appearing at $\pm 3\beta$ and $\pm 5\beta$. The new design should have a diffraction angle of approximately 3.5°, and this angle was used in the present study to examine fiber damage characteristics.

4.2 Grating Performance

The first two elements were used originally for single-fiber injection, and their characteristics have been reported previously.^{12,18} When used with our test laser (described in the next section), they produce a beam profile at the focal plane of the primary lens as shown in Fig. 7. The beam profile was recorded using a CCD camera (Silicon Mountain Design Model SMD-1M15) and beam-profiling software (Spiricon Model LBA-500PC Laser Beam Analyzer). The circle shown in this figure has a diameter of 365 μm , corresponding to the core diameter of the fibers used in past and present studies. The beam-profiling system can provide the ratio of the peak local fluence to the average fluence within this diameter. In previous testing to determine laser-induced damage characteristics,¹² this ratio was found to have an average value of 2.96 with a standard deviation of ± 0.07 . Fig. 8 shows the beam profiles produced at the focal plane of the primary lens when the diffractive grating is included. The particular grating position resulted in a 0.65 mm spacing between profiles. The lenslet array was rotated relative to its position when Fig. 7 was recorded, and the resulting hexagonal patterns in the focal plane shown in Fig. 8 are rotated accordingly. The beam profiles in the \pm first orders are duplicates of the zero order profile, except that their total energies are reduced. Using the beam-profiling system to compare energies within a 365- μm aperture at each location, the profiles on the left and right have 81% and 79% of the central profile energy, respectively.

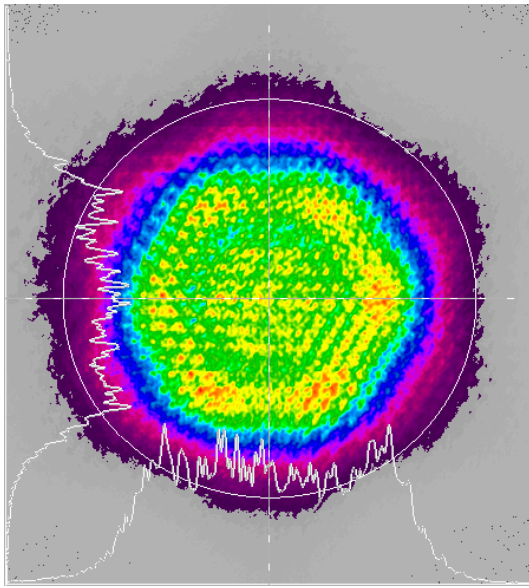


Fig. 7 Beam profile at a fiber entrance face using only the lenslet array and primary lens. The circle shown has a diameter of 365 μm .

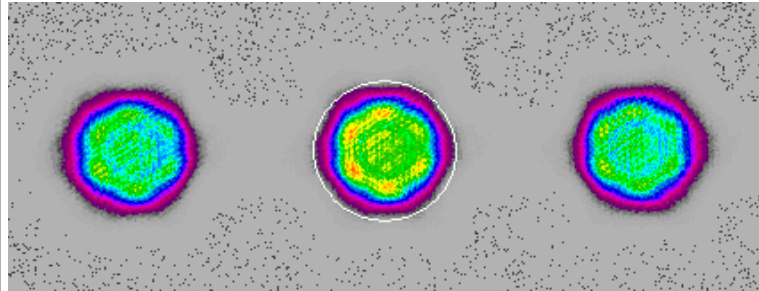


Fig. 8 Beam profiles at the focal plane of the primary lens with the grating beamsplitter in place. A circle with a diameter of 365 μm is shown around the center profile.

To measure the relative energies in different orders more carefully, a CW Nd:YAG laser operating at 1064 nm was used with the grating alone. An optical rail was mounted perpendicular to the undiffracted laser path 0.5 m from the grating. A power meter that could be rotated to point directly at the grating was traversed along the rail to record the power in each order. Repeated measurements showed that 32.5-32.7% of the incident power was in the zero order beam, 26.7-27.0% was in each of the first order beams, 2.7% was in each of the third order beams, and 0.8% was in each of the fifth order beams (Fig. 6). The overall efficiency for incident light transmitted into the zero and first orders was 86%.

4.2 Laser-induced damage characteristics

The beam axis for the zero order profile has normal incidence upon the center fiber, and this is identical to single-fiber injection. The experimental configuration that was used to examine laser-induced damage characteristics for single-fiber injection using the same lenslet array and primary lens¹² is shown in Fig. 9. This configuration is used again in the present study to examine the effects of injection angles introduced by the three-fiber injection optics. The test laser used in past and present studies is an oscillator-only, multimode Nd:YAG (Laser Photonics Model YQL-102) operated at the fundamental wavelength (1064 nm) in a Q-switched, single-shot mode. The maximum pulse energy available for fiber injection is 160 mJ. The average pulse width measured during the current study was 11.0 ns (FWHM), with a variation of ± 0.3 ns. This pulse width is somewhat longer than the 9.4 ns value measured during the previous single-fiber testing.

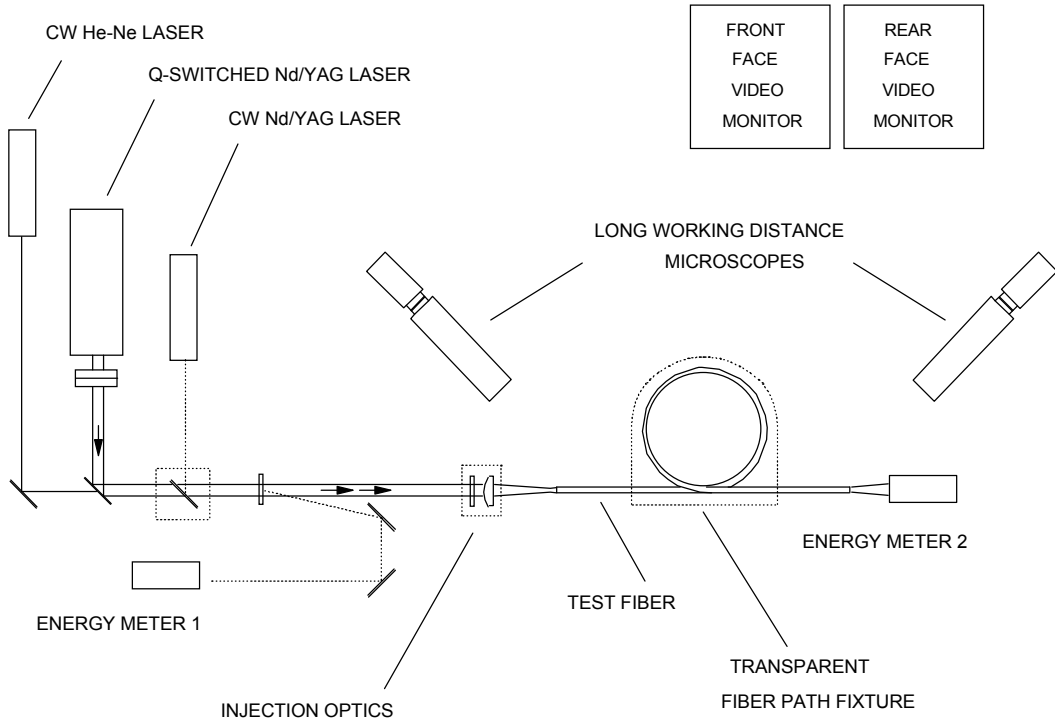


Fig. 9 Experimental configuration for fiber damage testing

Figure 10 shows the current near-field profile from this laser, recorded using the same beam-profiling system described previously. Figure 11 shows the laser beam incident on the lenslet array. Most of the beam energy is incident on a relatively small number of individual lenslets, and for most of these the incident fluence is not uniform over the lenslet area. The beam profile at the fiber entrance face with the current laser was shown in Fig. 7. During the present study, the ratio of peak fluence to average fluence over the fiber core area was found to have an average value of 2.95 and a standard deviation of 0.08. These fluence characteristics at the fiber entrance face are essentially the same as in the previous testing of single-fiber injection. As a measure of “spot size,” 86.5% of the total beam energy is within a diameter of 285 μm .

The fibers used in the present study were type FG400UER from InnovaQuartz, having a 365- μm diameter core of high-OH fused silica, a 17.5- μm thick cladding of F-doped fused silica (resulting in a numerical aperture of 0.22), a 12.5- μm thick TEQST™ hard polymer coating, and a 150- μm thick Tefzel® buffer. These fibers represent the currently available version of the 3M type FG-365-UER fiber used previously, and have essentially the same dimensions. Unlike previous studies, the fiber end faces were prepared by a commercial vendor using a proprietary polishing schedule following exceptionally good cleaving by Pioneer Optics. Although most fiber faces appeared free of scratches at high

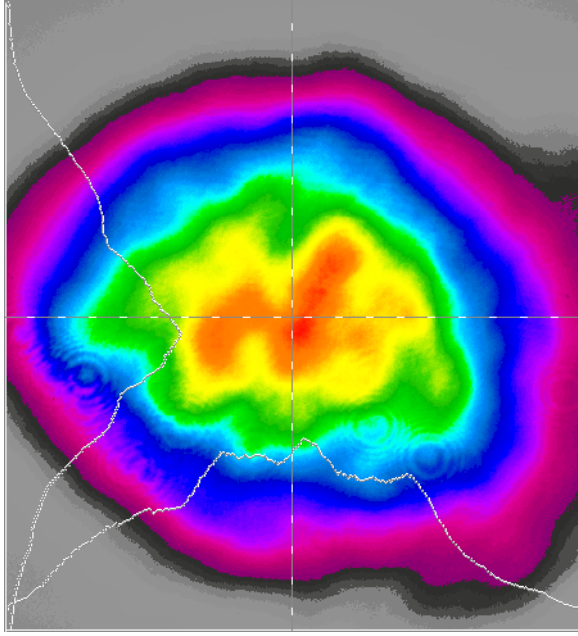


Fig. 10 Current near-field profile of the test laser. Line scans extend 6.3 mm in width and 7.2 mm in height

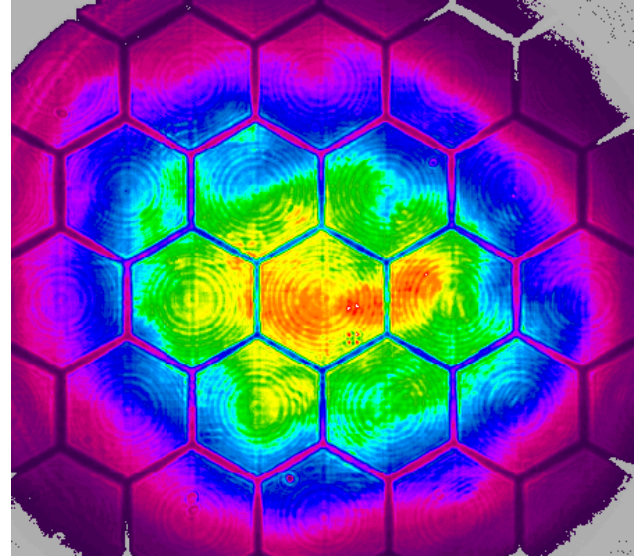


Fig. 11 Test laser incident on the lenslet array

magnification, the faces were very flat and many showed traces of the cleaving step, indicating that very little material was removed by the polishing schedule. Initial testing found that the entrance faces were likely to experience breakdowns at relatively low incident pulse energies, so an additional in-house polishing step using Syton HT-50 colloidal silica (South Bay Technology) was used for these faces. Consequences of the fiber face preparation will be discussed in Section 5.

The key question related to use of the three-fiber injection optics is whether the injection angle corresponding to the first order beams will have a detrimental effect on thresholds for laser-induced damage. An additional question is whether this angle results in significant energy injected into the cladding. To address these questions, the experimental configuration shown in Fig. 9 was modified to incorporate an angle between the incident laser beam axis and the axis of a fiber under test. In previous studies we used a custom fiber mount and careful alignment procedures in order to hold the entrance face of a test fiber within about 10 μm from the primary lens focal plane, and the fiber axis parallel to the beam axis to within 0.1°. The angle adjustment involved reflecting a He-Ne laser beam collinear with the Nd:YAG laser beam from an optical flat attached to the custom fiber mount over a distance of 1 m to ensure the adjustable yaw and pitch of the mount was correct. In the present study the mount was rotated so the reflected He-Ne beam would be offset 6.1 cm at the 1 m distance. This corresponds to the 3.5° diffraction angle anticipated for a new grating design, and represents a more severe condition than found with the prototype grating on hand (Section 4.1).

The maximum acceptance angle for the 0.22 NA fiber is 12.7°, and a 3.5° degree rotation of the fiber axis will result in a loss in transmission for some fraction of incident energy that exceeds an angle of 9.2° with respect to the laser beam axis (Fig. 4). A 9.2° angle and a focal length of 17.1 mm correspond to a beam diameter of 5.5 mm, and approximately 10% of the total beam energy (as shown in Fig. 10) is beyond this diameter. However, referring to Fig. 4, only incoming rays in the lower half of the beam whose in-plane component of the angle θ exceeds $(\alpha+\beta)$ will actually fail to be within the fiber's acceptance angle. Fiber transmission measurements that compared a 3.5° fiber rotation with a 0° rotation typically showed an additional transmission loss $\leq 1\%$ at the 3.5° angle. The transmission loss without fiber rotation is approximately 10% due to Fresnel reflection losses at both fiber faces and some overfilling of the core diameter by the beam profile at the fiber entrance face (Fig. 7).

A total of 20 test fibers were used to establish thresholds for laser-induced damage using the test configuration shown in Fig. 9 and a fiber rotation of 3.5° . The test procedure used for each fiber is illustrated in Fig. 12. After alignment using a very low pulse energy, the fiber was subjected to a series of single laser pulses in which the incident energy was increased with each successive pulse. The increments in pulse energy were smaller than in previous studies. The testing was halted when a breakdown or damage event occurred on a given shot. The maximum energy transmitted before this shot, and the attempted and actual transmitted energies during this shot, were then recorded. The collection of measured values for highest transmitted energy before breakdown or damage were then used to generate cumulative damage probability distributions.³ To represent the results in this fashion, the individual fiber data were first ordered from lowest to highest transmitted energy E_i before damage, then assigned a corresponding rank R_i , where $R_i = 1, 2, 3, \dots, 20$. The cumulative probability for damage F_i at energy E_i was then assigned according to:²³

$$F_i = (R_i - 0.5)/20$$

A Weibull distribution in terms of the variable E_i was obtained from a least-squares fit to the function:

$$F(E) = 1 - \exp[-(E/E_0)^m]$$

where m is the Weibull slope and E_0 is a scale parameter. The testing results and the corresponding Weibull distribution are shown in Fig. 13. The maximum energy transmitted before damage varied from 64 to 93 mJ. The transmitted energy

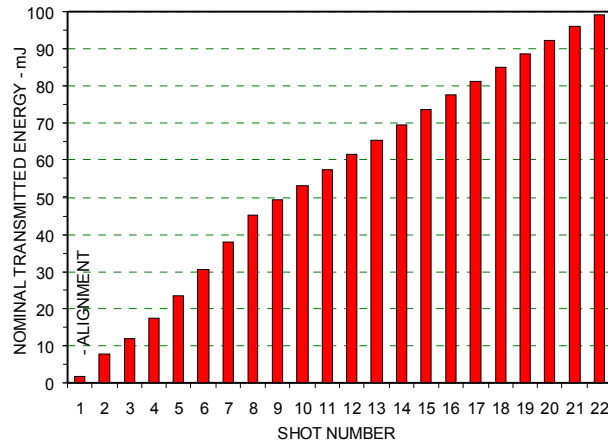


Fig. 12 Test sequence used for fiber damage testing

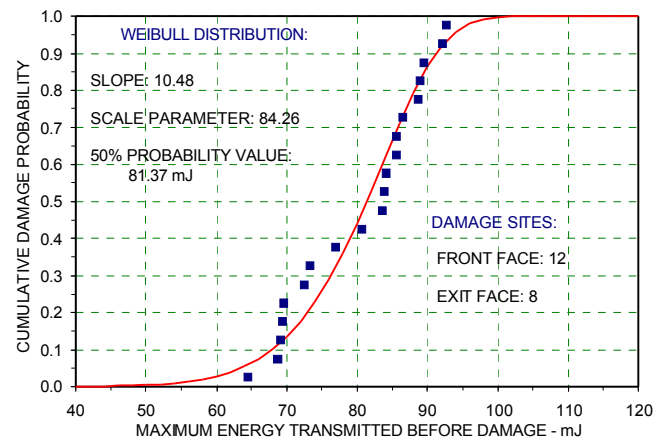


Fig. 13 Damage testing results with a 3.5° fiber axis rotation

corresponding to a 50% probability for damage was 81.4 mJ. Two different damage mechanisms were observed during this testing. The majority of fibers experienced entrance-face breakdown, resulting in a subtle damage pattern of small pits that mimicked the incident beam profile (Fig. 7). These were catastrophic damage events, as subsequent pulses would only result in stronger breakdowns and more pitting. The remainder of the fibers experienced exit-face damage. Four of the five fibers that damaged before transmitting 70 mJ experienced exit-face damage, with the remaining exit-face events occurring as high as 86 mJ. There were no fibers that experienced “entry” segment damage, either at the core/cladding interface or along the fiber axis. In contrast, when damage thresholds were examined using these injection optics for single-fiber injection,¹² a persistent “entry” damage mechanism was evident. The previous results are shown in Figs. 14 and 15. The only damage mechanisms observed were entrance-face breakdown and “entry” damage, with “entry” damage occurring in 9 of the 20 fibers tested. The two fibers that damaged at the lowest energies experienced this damage mechanism, with the remaining “entry” events uniformly scattered over the range of energies shown in Fig. 14. The locations of these damage sites relative to the fiber entrance face are sketched in Fig. 15. These sites were roughly centered within the fiber core, rather than near the core/cladding interface. The location of the damage sites near the fiber axis and the regular spacing shown in Fig. 15 indicate a radial refocusing pattern occurring within the “entry”

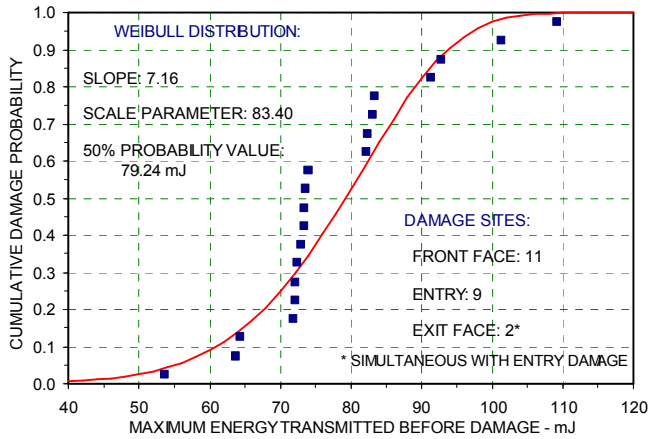


Fig. 14 Damage testing results for single-fiber injection (Ref. 12)



Fig. 15 Axial location of “entry” damage sites (Ref. 12)

segment. The present results indicate that this refocusing pattern was mitigated by injection with a 3.5° angle between the beam axis and the fiber axis.

For reference, the transmitted energies can be converted to incident fluence values. The Weibull fit shown in Fig. 13 gives a value of 81.4 mJ for a 50% damage probability. This transmitted pulse energy corresponds to approximately 88 mJ incident on the fiber core at the entrance face. With a core diameter of 365 μm , the average incident fluence would then be 84 J/cm^2 . The peak local fluence at the fiber entrance face would correspond to this value multiplied by the ratio of peak to average fluences at this location (~ 3.0).

5. DISCUSSION

As in a previous study of optics for single-fiber injection, the current testing used a hexagonal lenslet array and a primary lens with a 17.1 mm focal length. The fiber axis was rotated 3.5° from the incoming beam axis to examine damage threshold characteristics for fibers whose positions would correspond to the first diffraction order for a grating with this diffraction angle. The damage characteristics for the zero order fiber can be described by the previous testing using the same injection optics (Fig. 14) provided other test conditions were comparable. The ratios of the peak fluence to the average fluence over the fiber core area were essentially the same, but the laser pulse width was somewhat longer in the current testing. If the threshold fluence for surface damage is assumed to vary with pulse width to a 0.35 power,²⁴ the longer pulse width in the current testing would raise damage fluences by 5-6%. A more significant difference in test conditions could be due to the fiber end-face preparations used for the current study. Fibers in the previous study were mechanically polished in-house using a carefully developed schedule following very good cleaving.¹² Fibers in the current study were polished by a commercial vendor following the same cleaving process. Conditioning with a CO₂ laser was not done in either study. Although most of the current fiber faces were free of scratches under high magnification, they were much flatter than the faces in the previous testing and many showed evidence of the cleaving step. This indicates that very little material had been removed during the polishing. An additional in-house polishing step using colloidal silica was added to the entrance faces to improve their resistance to breakdown, and the distribution of energies for entrance-face breakdowns in the current study was comparable to that found in the previous study. However, such an additional polishing step would have no benefit for the exit faces. As mentioned previously, exit-face damage is due to subsurface defects which can be a consequence of cleaving as well as early polishing steps. If sufficient material is not removed during subsequent polishing steps, these defects will remain and can be dominant damage sites. This was the case in the current testing, with exit-face damage occurring in 8 out of 20 fibers. As a consequence, the observation of other damage mechanisms with higher thresholds may not have been possible.

Despite the poor exit-face preparation, the Weibull distribution fit to the current test results still shows a higher slope and a slightly higher energy for a 50% damage probability. Although the longer pulse width provides some benefit, the

primary reason for better threshold characteristics is the absence of on-axis “entry” damage observed in 9 out of 20 fibers during the previous testing. Injection with a 3.5° angle between the beam axis and the fiber axis apparently mitigates the refocusing pattern that produces this damage when the beam axis is closely collinear with the fiber axis. In addition, the 3.5° angle produced a relatively small effect on transmission efficiency, indicating that little additional energy was being injected into the cladding. Finally, the absence of “entry” damage at the core/cladding interface indicates that the refocusing pattern that would be expected with “low NA” injection at this angle was mitigated by the beam-shaping element and the short focal length of the primary lens.

Considering both past and present results, a reasonable assessment can be made of fiber damage characteristics for the three-fiber injection optics under consideration. Assuming that better procedures are followed for fiber face preparation, “entry” damage along the axis of the center fiber is likely to be the limiting mechanism that determines system margins with respect to laser-induced damage. This is certainly true for the prototype grating that results in nearly 20% more energy in the zero order, but probably would be true even with an improved grating design that provides better energy balance. Nevertheless, these injection optics should provide useful margins if nominal transmitted pulse energies are well below the values shown in Fig. 14.

Although laser injection into three parallel fibers is a relatively simple case, the evaluation of the present design illustrates the additional challenges that can arise in trying to achieve high damage thresholds during multiple-fiber injection. The design of optics for high-intensity laser injection into greater numbers of fibers will likely find these challenges more difficult to address.

ACKNOWLEDGMENTS

Sandia is a multiprogram laboratory operated by Sandia Corporation, a Lockheed Martin Company, for the United States Department of Energy’s National Nuclear Security Administration under Contract DE-AC04-94AL85000.

REFERENCES

1. J. A. Harrington, “An Overview of Power Delivery and Laser Damage in Fibers,” Proc. SPIE 2966, 536 (1997). Also: the nine following papers in Proc. SPIE 2966.
2. For example, see papers in Optical Technologies for Arming, Safing, Fuzing, and Firing I and II, edited by William J. Thomes, Jr. and Fred M. Dickey, Proc. of SPIE Vols. 5871 (2005) and 6287 (2006).
3. R. E. Setchell, “An Optimized Fiber Delivery System for Q-switched, Nd:YAG Lasers,” Proc. SPIE 2966, 608 (1997). Also: earlier references cited within.
4. R. E. Setchell, “Laser-Induced Damage in Step-Index, Multimode Fibers,” Proc. SPIE 1848, 15 (1993).
5. R. E. Setchell, “End-face Preparation Methods for High-Intensity Fiber Applications,” Proc. SPIE 3244, 390 (1998).
6. R. E. Setchell, “Effects of Accelerated Aging on Fiber Damage Thresholds,” Proc. SPIE 3578, 743 (1999).
7. D. Gloge, “Optical Power Flow in Multimode Fibers,” Bell Syst. Tech. J. 51, 1767 (1972).
8. S. W. Allison, G. T. Gillies, D. W. Magnuson, and T. S. Pagano, “Pulsed Laser Damage to Optical Fibers,” Appl. Opt. 24, 3140 (1985).
9. R. Pini, R. Salimbeni, and M. Vannini, “Optical Fiber Transmission of High Power Excimer Laser Radiation,” Appl. Opt. 26, 4185 (1987).
10. W. M. Trott and K. D. Meeks, “High-Power Nd:Glass Laser Transmission Through Optical Fibers and Its Use in Acceleration of Thin Foil Targets,” J. Appl. Phys. 67, 3297 (1990).

11. A. W. Snyder and J. D. Love, Optical Waveguide Theory, Chapman and Hall, London, 1983, pp.180-188.
12. R. E. Setchell, "Laser Injection Optics for High-Intensity Transmission in Multimode Fibers," Proc. SPIE 4095, 74 (2000).
13. R. E. Setchell and P. Klingsporn, "Laser-Induced Damage Studies on Step-Index, Multimode Fibers," Proc. SPIE 1624, 56 (1992).
14. R. E. Setchell, K. D. Meeks, W. M. Trott, P. Klingsporn, and D. M. Berry, "High-Power Transmission Through Step-Index, Multimode Fibers," Proc. SPIE 1441, 61 (1991).
15. N. L. Boling, M. D. Crisp, and G. Dube, "Laser Induced Surface Damage," Appl. Opt. 12, 760 (1973).
16. W. C. Sweatt and M. W. Farn, "Kinoform/Lens System for Injecting a High Power Laser Beam Into an Optical Fiber," Proc. SPIE 2114, 82 (1994).
17. R. E. Setchell, "Damage Studies in High-Power Fiber Transmission Systems," Proc. SPIE 2114, 87 (1994).
18. L. S. Weichman, F. M. Dickey, and R. N. Shagam, "Beam Shaping Element for Compact Fiber Injection Systems," Proc. SPIE 3929, 176 (2000).
19. P. D. Sundvold and W. B. Hageman, "Optical Firing System," Proc. SPIE 5871, 587104 (2005).
20. A. M. Frank, P. R. Wilkins, J. Honig, M. Moss, and C. Gillespie, "High Energy Laser Pulse Multiplexing into a Fused Silica Fiber Array," Proc. SPIE 4095, 85 (2000).
21. J. Honig, "A 1-Joule Laser for a 16-Fiber Injection System," Proc. SPIE 4095, 98 (2000).
22. D. M. Brown, F. M. Dickey, and W. J. Thomas, Jr., "Design Considerations for Multi-Fiber Injection," Proc. SPIE 5871, 587106 (2005).
23. B. Bergman, "On the Estimation of the Weibull Modulus," J. Mater. Sci. Lett. 3, 689 (1984).
24. F. Ranier, L. J. Atherton, J. H. Campbell, F. D. De Marco, M. R. Kozlowski, A. J. Morgan, and M. C. Staggs, "Four-Harmonic Database of Laser-Damage Testing," Proc. SPIE 1624, 116 (1992).